

EFFECT OF SAMPLING RATES ON THE PERFORMANCE OF MODEL-BASED CONTROL SCHEMES

Pradeep K. Khosla

Department of Electrical and Computer Engineering
The Robotics Institute
Carnegie-Mellon University
Pittsburgh, PA 15213

Abstract

In our previous research, we experimentally implemented and evaluated the effect of dynamics compensation in model-based control algorithms. In this paper, we evaluate the effect of changing the control sampling period on the performance of the computed-torque and independent joint control schemes. While the former utilizes the complete dynamics model of the manipulator, the latter assumes a decoupled and linear model of the manipulator dynamics. We discuss the design of controller gains for both the computed-torque and the independent joint control schemes and establish a framework for comparing their trajectory tracking performance. Our experiments show that within each scheme the trajectory tracking accuracy varies slightly with the change of the sampling rate. However, at low sampling rates the computed-torque scheme outperforms the independent joint control scheme.

1. Introduction

Although many simulation results have been presented^{1, 2, 3}, the real-time implementation and performance of model-based control schemes with high control sampling rates had not been demonstrated on actual manipulators, until recently^{4, 5, 6}. The main reasons for this have been the lack of a suitable manipulator system and the fact that it is difficult to evaluate the dynamics parameters for implementing model-based algorithms. One of the goals of the CMU Direct-Drive Arm II⁷ project has been to overcome these difficulties and evaluate the effect of dynamics compensation on the real-time trajectory tracking of manipulators. For the real-time Computation of the inverse dynamics, we have developed a high-speed and powerful computational environment. The computation of inverse dynamics has been customized for the CMU DD Arm II and a computation time of 1 *ms* has been achieved⁸. To obtain an accurate model we have computed and measured the various parameters from the engineering drawings of the CMU DD Arm II by modeling each link as a composite of hollow and solid cylinders, prisms, and rectangular parallelpipeds. We have also proposed an algorithm to identify the dynamics parameters⁹ which has been implemented on the CMU DD Arm II. The results of the experimental implementation of our identification algorithm are presented in¹⁰. Finally, the negligible friction in our directdrive arm makes it suitable to test the efficacy of the computed-torque scheme.

Based on the above contributions, in our previous research, we investigated the effect of high sampling rate dynamics compensation in model-based manipulator control methods.

Specifically, we compared the computed-torque scheme which utilizes the complete dynamics model of the manipulator with the independent joint control scheme⁴ and the feedforward compensation method¹¹. The control schemes were implemented on the CMU DD Arm II with a sampling period of 2 ms.

In this paper, we investigate the effect of reducing the sampling rate on the trajectory tracking performance of model-based manipulator control methods. We first compare the performance of each scheme as the sampling rate is changed. Next, we also compare the relative performance of both the computed-torque and the independent joint control schemes at different sampling rates. Our work represents the first experimental evaluation of the effect of the sampling rate on the performance of both the computed-torque and the independent joint control schemes. We discuss the design of the controller gains for both the independent joint control and the computed-torque schemes and establish a framework for the comparison of their trajectory tracking performance. Our experiments demonstrate that the computed-torque scheme exhibits a better performance than the independent joint control scheme. Our experiments also show that high sampling rates are important because they result in a stiffer system that is capable of effectively rejecting unknown external disturbances.

This paper is organized as follows: In Section 2, we describe previous research in manipulator control and provide a motivation for our work. Then in Section 3, we present an overview of the manipulator control schemes that have been implemented and evaluated on the CMU DD Arm II. The design of controllers is discussed in Section 4 and the real-time experimental results are presented and interpreted in Section 5. Finally, in Section 6 we summarize this paper. In the Appendix, we describe our experimental hardware set-up.

2. Past Work and Motivation

The robot control problem revolves around the computation of the actuating joint torques/forces to follow the desired trajectory. The dynamics of a manipulator are described by a set of highly nonlinear and coupled differential equations. The complete dynamic model of an N degrees-of-freedom manipulator is described by:

$$\tau = D(\theta)\ddot{\theta} + h(\theta, \dot{\theta}) + g(\theta) \quad (1)$$

where τ is the N -vector of the actuating torques; $D(\theta)$ is the $N \times N$ position dependent manipulator inertia matrix; $h(\theta, \dot{\theta})$ is the N -vector of Coriolis and centrifugal torques; $g(\theta)$ is the N -vector of gravitational torques; and $\ddot{\theta}$, $\dot{\theta}$ and θ are N -vectors of the joint accelerations, velocities and positions, respectively.

This complex description of the system makes the design of controllers a difficult task. To circumvent the difficulties the control engineer often assumes a simplified model to proceed with the controller design. Industrial manipulators are usually controlled by conventional PID-type independent joint control structures designed under the assumption that the dynamics of the links are uncoupled and linear. The controllers based on such an overly simplified dynamics model result in low speeds of operation and overshoot of the end-effector.

To improve the performance of the PID controllers, researchers have investigated model-based control schemes which attempt to compensate for the nonlinearities and the mismatch in the dynamical description of the robot. One of the model-based techniques is the feedforward dynamics compensation method which computes the desired torques from the given trajectory and injects these torques as feedforward control signals. Independent joint feedback controllers are then added with the intention of compensating

for the small coupling torques arising out of the mismatch in the dynamics of the model and the real arm'. More thorough compensation is achieved by the computed-torque technique in which the dynamics model is included in the feedback loop to decouple and linearize the manipulator dynamics. This technique has **also** been extended to operate in the Cartesian space and is called **resolved-acceleration** scheme².

One of the fundamental problems with real-time dynamics compensation has been the high computational requirements of the inverse dynamics formulations. This drawback led researchers to evaluate the significance of the terms in the dynamical model and compensate only for the significant terms. Another avenue that was explored involved the use of table look-up and interpolation techniques¹². Recently there has been much work in reducing the computational requirements based on the structure of the dynamical equations^{13, 14}. Further, high speed controller architectures have **also** been proposed and demonstrated⁸. These developments have made it possible to experimentally implement and evaluate the nonlinear model-based control schemes^{4, 5}.

Several researchers have followed an entirely different avenue of research that involves looking at alternate controllers that are computationally less expensive than the model-based schemes and at the same time robust. This has led to the development of alternate methods such as linear multivariable control¹⁵, self-tuning and model-reference adaptive control^{16, 17}, sliding control¹⁸, and prediction control¹⁹.

Real-Time digital implementation of either model-based schemes or alternate control schemes requires the designer to make a choice of the sampling rate. Thus it is important to develop both theoretical and experimental methods to evaluate the effect of sampling rates on the performance of manipulator control methods. A theoretical investigation in this area is still an uncharted territory probably due to the nonlinear and coupled nature of the manipulator dynamics. In this paper, however, we present experimental results on evaluating the effect of changing the sampling rates on the performance of independent joint control and computed-torque schemes. A similar evaluation for alternate control schemes (as presented above) is beyond the scope of this paper and is a topic of current investigation. In the next section, we describe the control schemes that have been implemented on the CMU DD Arm II.

3. Schemes Implemented

We have implemented computed-torque and the independent joint control schemes and compared their real-time performance as a function of the control sampling rate. These schemes are described in the sequel.

Independent Joint Control (IJC)

In this scheme linear PD control laws were designed for each joint based on the assumption that the joints are decoupled and linear. The control torque τ applied to the joints at each sampling instant is:

$$\tau = \mathbf{J}\mathbf{u}_i \quad (2)$$

where \mathbf{J} is the constant $N \times N$ diagonal matrix of link inertias at a typical position, and \mathbf{u}_i is the vector of commanded accelerations.

This scheme utilizes nonlinear feedback to decouple the manipulator. The control torque τ is computed by the inverse dynamics equation in (1), using the commanded acceleration \mathbf{u}_i instead of the measured acceleration $\ddot{\theta}$:

$$\tau = \hat{\mathbf{D}}(\theta)\mathbf{u}_i + \hat{\mathbf{h}}(\theta, \dot{\theta}) + \hat{\mathbf{g}}(\theta) \quad (3)$$

where the $\hat{\cdot}$ indicates that the estimated values of the dynamics parameters are used in the computation.

Before proceeding with a meaningful comparison of the performance of the computed-torque and the independent joint control schemes it is necessary to establish a common framework. In order to achieve this, we consider the control law in two steps; computation of the commanded acceleration and computation of the control torque. The commanded joint accelerations u_i can be computed in one of the following three ways:

$$u_1 = K_p(\theta_d - \theta) - K_v \dot{\theta} \quad (4)$$

$$u_2 = K_p(\theta_d - \theta) + K_v(\dot{\theta}_d - \dot{\theta}) \quad (5)$$

$$u_3 = K_p(\theta_d - \theta) + K_v(\dot{\theta}_d - \dot{\theta}) + \ddot{\theta}_d \quad (6)$$

where K_p and K_v are $N \times N$ diagonal position and velocity gain matrices, respectively. The N -vectors θ_d and θ are the desired and measured joint positions, respectively, and the $\dot{\cdot}$ indicates the time derivative of the variables. Whereas only the position error and the velocity damping is used in (4), the commanded acceleration signal in (5) uses a velocity feedforward term, and the commanded acceleration signal in (6) uses both the velocity and acceleration feedforward terms. The idea is to increase the speed of response by incorporating a feedforward term.

The fundamental difference between the independent joint control schemes and the model-based schemes lies in the second step in the control law, i.e., the method of computing the applied control torque signals from the commanded acceleration signals. If the vector of actuating joint torques τ is computed from the commanded acceleration signal under the assumption that the joint inertias are constant, then we obtain an independent joint control scheme. On the other hand, if the actuating torques τ are computed from the inverse **dynamics** model in (1) then we obtain the computed-torque scheme.

We have performed real-time experiments and evaluated the effect of changing the sampling rates on the performance of the independent joint control and the computed-torque schemes. The experiments were performed on the **CMU DD Arm II**. In our experiments, we have used Equation 6 to compute the accelerations for both the computed-torque and the independent joint control schemes. In the next section, we explain our procedure to determine the gain matrices for both the computed-torque and the independent joint control schemes.

4. Controller Design

The performance of the nonlinear CT scheme and the linear **IJC** scheme can be compared only if the same criteria are used for design of the controller gain matrices. Fortunately, this is possible because the gain matrices K_p and K_v appear only in the commanded accelerations (Equations (4)-(6)) which are the same for both CT and **IJC** schemes. Thus, whether we implement the simplistic independent joint control scheme or the sophisticated computed-torque scheme, we are faced with the problem of designing the gain matrices K_p and K_v . These matrices are chosen to satisfy the specified output response criterion.

4.1. Design of Gain Matrices for Independent Joint Control

The closed loop transfer function relating the input θ_{jd} to the measured output θ_j for joint j is:

$$\frac{\theta_j}{\theta_{jd}} = \frac{s^2\delta + s\gamma k_{vj} + k_{pj}}{s^2 + k_{vj}s + k_{pj}} \quad (7)$$

where $\gamma=1$ if velocity feedforward is included and zero otherwise, and $\delta=1$ if acceleration feedforward is included and zero otherwise. The closed-loop characteristic equation in all the three cases is,

$$s^2 + k_{vj}s + k_{pj} = 0 \quad (8)$$

and its roots are specified to obtain a stable response. The complete closed-loop response of the system is governed by both the zeros and the poles of the system. In the absence of any feedforward terms, the response is governed by the poles of the transfer function.

Since it is desired that none of the joints overshoot the commanded position or the response be critically damped, our choice of the matrices K_p and K_v must be such that their elements satisfy the condition:

$$k_{vj} = 2\sqrt{k_{pj}} \quad \text{for } j = 1, \dots, 6 \quad (9)$$

Besides, in order to achieve a high disturbance rejection ratio or high stiffness it is also necessary to choose the position gain matrix K_p as large as possible which results in a large K_v .

4.2. Design of Gain Matrices for Computed-Torque Scheme

The basic idea behind the computed-torque scheme is to achieve dynamic decoupling of all the joints using nonlinear feedback. If the dynamic model of the manipulator is described by (1) and the applied control torque is computed according to (3), then the following closed-loop system is obtained:

$$\ddot{\theta} = u_i - [D]^{-1}\{[D - \dot{D}]\dot{\theta} + [h - \dot{h}] + [g - \dot{g}]\}$$

where the functional dependencies on θ and $\dot{\theta}$ have been omitted for the sake of clarity. If the dynamics are modeled exactly, that is, $\dot{D}=D$, $\dot{h}=h$ and $\dot{g}=g$, then the decoupled closed loop system is described by

$$\ddot{e} = u_i$$

Upon substituting the right hand side of either (4), (5) or (6) in the above equation, we obtain the closed-loop input-output transfer function of the system. The closed-loop characteristic equation in all the three cases is:

$$s^2 + k_{vj}s + k_{pj} = 0 \quad (10)$$

where k_{vj} and k_{pj} are the velocity and position gains for the j -th joint. Upon comparing (8) and (10), we obtain the relationships

$$k_{pj}^{[CT]} = k_{pj}^{[IJC]} \quad \text{and} \quad k_{vj}^{[CT]} = k_{vj}^{[IJC]}$$

which suggest that the gains of the IJC scheme are also the gains of the CT scheme. This equality must be expected because the closed-loop characteristic equation for both the independent joint control and the computed-torque scheme is the same.

4.3. Gain Selection

The gain matrices K_p and K_v are a function of the sampling rate of the control system²⁰. The higher the sampling rate the larger the values of K_p and K_v that can be chosen. Since the stiffness (or disturbance rejection property) of the system is governed by the position gain matrix (K_p) a higher sampling rate implies higher stiffness also. In practice the choice of the velocity gain K_v is limited by the noise present in the velocity measurement. We determined the upper limit of the velocity gain experimentally: we set the position gain to zero and increased the velocity gain of each joint until the unmodeled high-frequency dynamics of the system were excited by the noise introduced in the velocity measurement. This value of K_v represents the maximum allowable velocity gain. We chose 80% of the maximum velocity gain in order to obtain as high value of the position gain as possible and still be well within the stability limits with respect to the unmodeled high frequency dynamics. The elements of the position gain matrix K_p were computed to satisfy the critical damping condition in (9) and also achieved the maximum disturbance rejection ratio. The elements of the velocity and position gain matrices (chosen for a sampling rate of 500 Hz) that were used in the implementation of the control schemes are listed in Table 1. The above procedure was repeated to select the gain matrices for sampling rates ranging from 500 Hz to 200 Hz.

5. Experiments and Results

In our experiments we implemented both the independent joint control scheme and the computed-torque scheme. We evaluated their individual and relative performances by changing the sampling rate but keeping both the position and the velocity gain matrices fixed. The maximum permissible velocity and position gains were chosen at a control sampling period of 5 ms (according to the method outlined in Section 4.3) and remained fixed even when the sampling period was changed. This allows us to determine the effect of the sampling rate on the trajectory tracking control performance. We have also evaluated the best performance of the CT method for a sampling period of 2 ms with its best performance for a sampling period of 5 ms. We conducted the evaluation experiments on a multitude of trajectories but due to space limitations we present our results for a simple but illustrative trajectory.

The first trajectory is chosen to be simple and relatively slow but capable of providing insight into the effect of dynamics compensation. In this trajectory only joint 2 moves while all the other joints are commanded to hold their zero positions and can be envisioned from the schematic diagram in Figure 1. Joint 2 is commanded to start from its zero position and to reach the position of 1.5 rad in 0.75 seconds; it remains at this position for an interval of 0.75 seconds after which it is required to return to its home position in 0.75 seconds. The points of discontinuity, in the trajectory, were joined by a fifth-order polynomial to maintain the continuity of position, velocity and acceleration along the three segments. The desired position, velocity and acceleration trajectories for joint 2 are depicted in Figure 2. The maximum velocity and acceleration to be attained by joint 2 are 2 rad/sec and 6 rad/sec², respectively.

The position tracking performance of joint 2 for both the CT and IJC schemes, for a control sampling rate of 200 Hz (corresponding to a control sampling period of 5 ms), is depicted in Figure 3. The corresponding position and velocity tracking errors are presented in Figures 4 and 5, respectively. We also depict the position tracking error of joint 1 in Figure 6 for both the CT and IJC schemes. We note that the CT scheme outperforms the IJC scheme. For example, in the case of joint 2 the maximum position tracking error for CT scheme is 0.03 rads while for the IJC scheme it is 0.45 rads, approximately. In an

earlier paper⁴, we had compared both the CT and IJC schemes with a control sampling period of 2 ms. It must be noted that in the earlier reported experiments' the gains were selected for a control sampling period of 2 ms whereas in the present experiments the gains have been selected for a control sampling period of 5 ms. To put the results in perspective, we recall that in the earlier experiment the maximum position tracking error for the CT method was 0.022 rads while for the IJC method it was 0.036 rads. From the above observations it may be deduced that increasing the control sampling period from 2 to 5 ms results in a noteworthy degradation of the performance of the IJC scheme. A similar increase in the sampling rate also improves the performance of the CT scheme.

In Figure 7, we depict the performance of the CT scheme as the sampling rate is increased from 200 Hz to 500 Hz. In this case the position and velocity gain matrices were determined for a sampling rate of 200 Hz and they remained fixed even when the sampling rate was increased to 500 Hz. Thus, Figure 7 presents the relative performance of the CT method as a function of the sampling rate only. We note that the trajectory tracking performance for both 200 Hz and 500 Hz sampling rates is comparable and has not changed in any appreciable manner with an increase in the sampling rate. Figure 8 depicts the results for the IJC method when a similar experiment was performed. In this case also we do not observe any appreciable change in performance when only the sampling rate is changed.

Thus, from the above set of experiments the following conclusions may be drawn:

1. If the gains are selected for a lower sampling rate and then if the sampling rate is increased: while keeping the gains fixed, there is no appreciable improvement in the performance of both the CT and the IJC schemes.
2. At lower sampling rates the CT scheme outperforms the IJC method. Even though the disturbance rejection ratio of both the schemes is diminished, it does not appreciably affect the CT method because of the compensation for the nonlinear and coupling terms. Whereas it affects the IJC method because the disturbance that is constituted by the nonlinear and the coupling terms is not rejected appreciably.
3. If the maximum possible gains are selected for the chosen sampling rates then the performance of CT at a higher sampling rate is better than its performance at a lower sampling rate. A similar conclusion is drawn for the IJC scheme also.

Our last conclusion is especially significant because it suggests that a higher sampling rate does not only imply improved performance but it also allows us to achieve high stiffness. It is desirable for a manipulator to have high stiffness so that the effect of unpredictable external disturbances on the trajectory tracking performance is significantly reduced.

6. Summary

In this paper, we have presented the first experimental evaluation of the effect of the sampling rate on the performance of both the computed-torque and the independent joint control schemes. We have discussed the design of the controller gains for both the independent joint control and the computed-torque schemes and established a framework for the comparison of their trajectory tracking performance. Based on our experiments we have demonstrated that the computed-torque scheme exhibits a better performance than

the independent joint control scheme. Our experiments also show that high sampling rates are important because they result in a stiffer system that is capable of effectively rejecting unknown external disturbances.

7. Acknowledgements

This research was supported in part by the National Science Foundation under Grant ECS-8320364 and the Department of Electrical and Computer Engineering, Carnegie Mellon University. The author acknowledges the cooperation of Prof. Takeo Kanade (Head of Vision Laboratory, Carnegie Mellon University) throughout the course of this research.

I. The CMU DD Arm II

We have developed, at CMU, the concept of directdrive robots in which the links are directly coupled to the motor shaft. This construction eliminates undesirable properties like friction and gear backlash. The CMU DD Arm II⁷ is the second version of the CMU directdrive manipulator and is designed to be faster, lighter and more accurate than its predecessor CMU DD Arm I²¹. We have used brushless rare-earth magnet DC torque motors driven by current controlled amplifiers to achieve a torque controlled joint drive system. The SCARA-type configuration of the arm reduces the torque requirements of the first two joints and also simplifies the dynamic model of the arm. To achieve the desired accuracy, we use very high precision (16 bits/rotation) rotary absolute encoders. The arm weighs approximately 70 pounds and is designed to achieve maximum joint accelerations of 10 rad/sec².

The hardware of the DD Arm II control system consists of three integral components: the Motorola M68000 microcomputer, the Maripco processor and the TMS-320 microprocessor-based individual joint controllers. We have also developed the customized Newton-Euler equations for the CMU DD Arm II and achieved a computation time of 1 ms by implementing these on the Maripco processor. The details of the customized algorithm, hardware configuration and the numerical values of the dynamics parameters are presented in 8.

Joint (j)	Transfer Function ($\frac{-1}{J_j s^2}$)	k_{pj}	k_{vj}
1	$\frac{1}{12.3s^2}$	2.75	3.33
2	$\frac{1}{2s^2}$	15.0	7.5
3	$\frac{1}{0.25s^2}$	256.0	32.0
4	$\frac{1}{0.007s^2}$	1285.0	71.5
5	$\frac{1}{0.006s^2}$	625.0	50.0
6	$\frac{1}{0.0003s^2}$	1110.0	50.0

Table 1: Transfer Functions and Gains of Individual Links

Figure 1: Schematic Diagram of 3 DOF DD Arm II

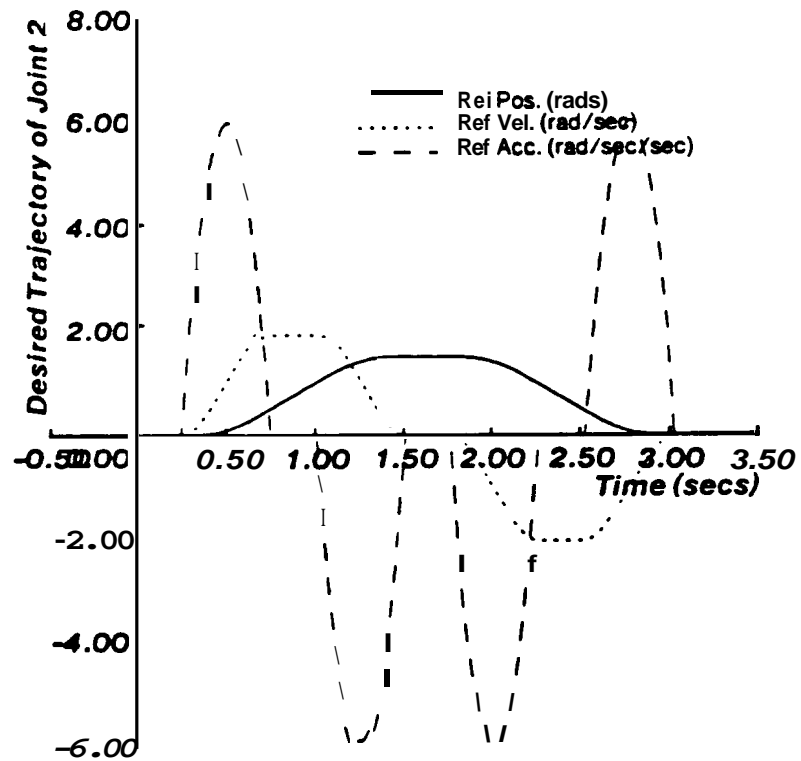
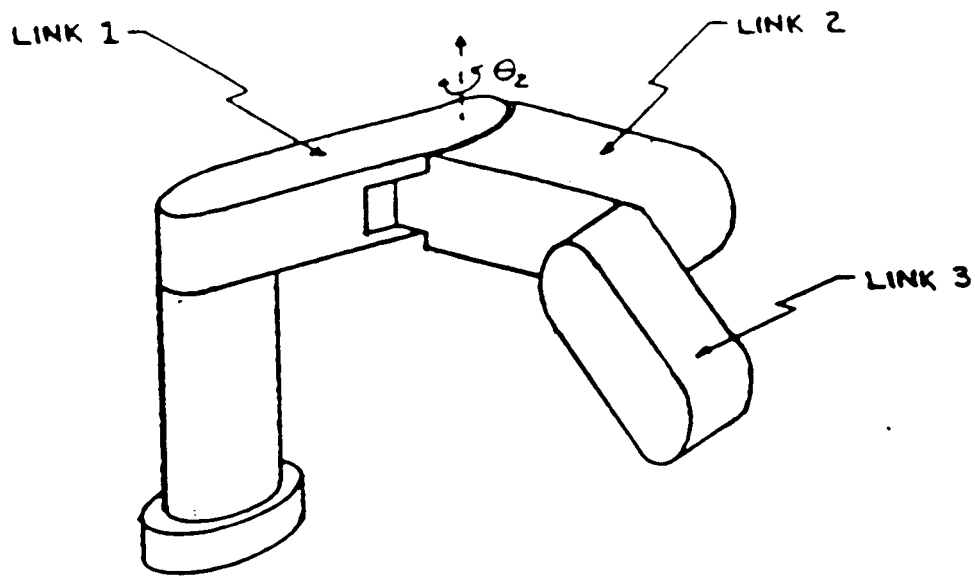


Figure 2: Desired Trajectories for Joint 2

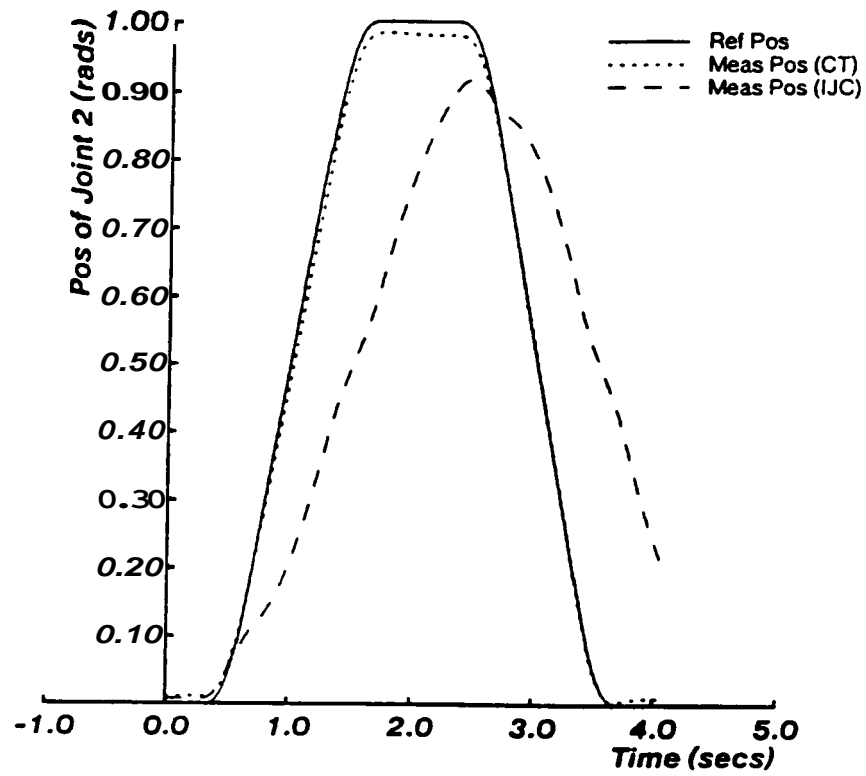


Figure 3: Position Tracking of CT and IJC at 5 ms Sampling

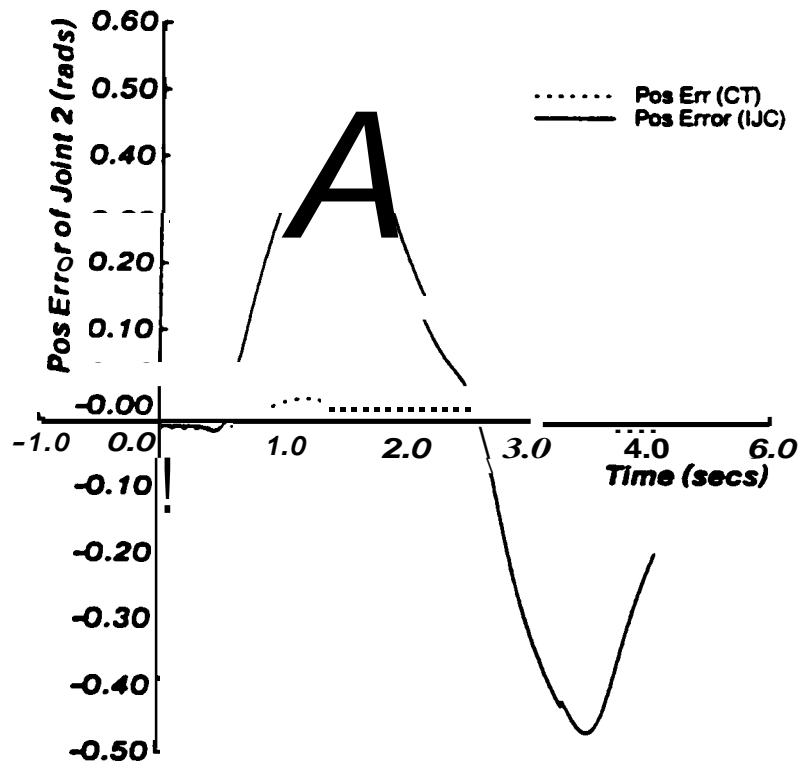


Figure 4: Position Tracking Error of Joint 2

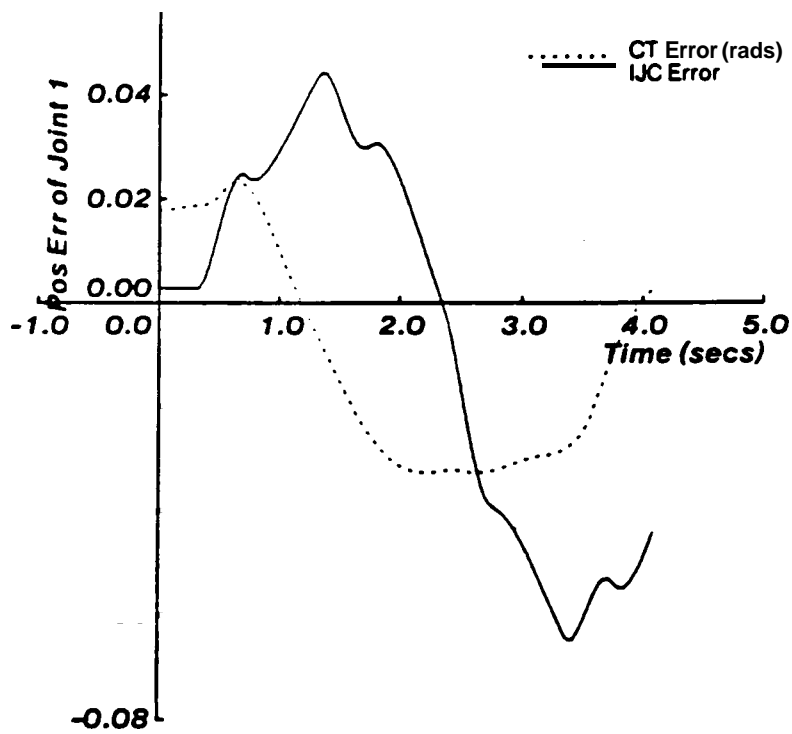
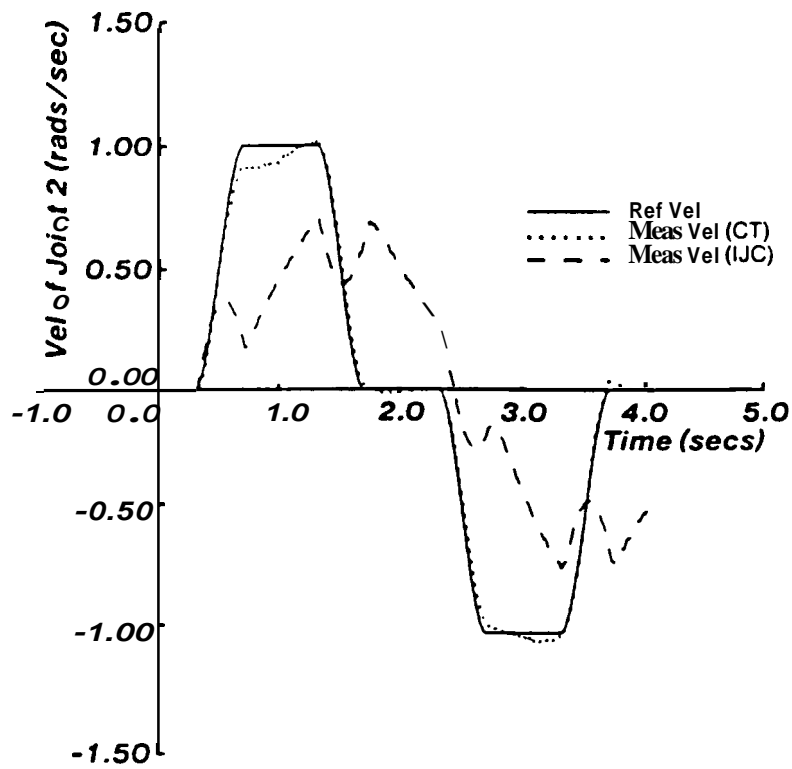


Figure 6: Position Tracking Errors of Joint 1

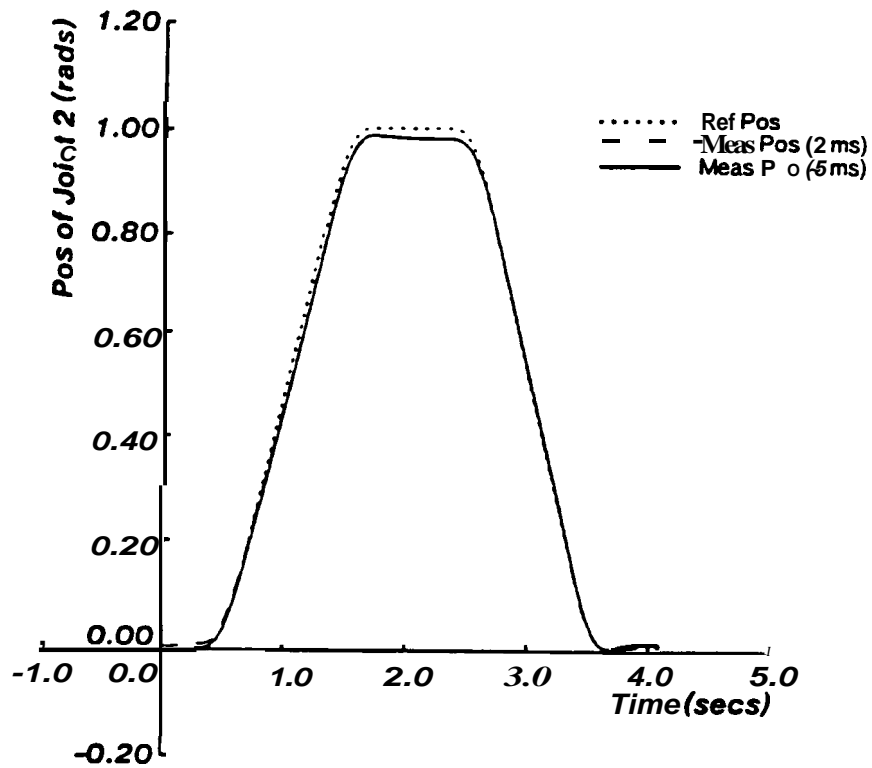


Figure 7: Performance of CT as a Function of Sampling Period

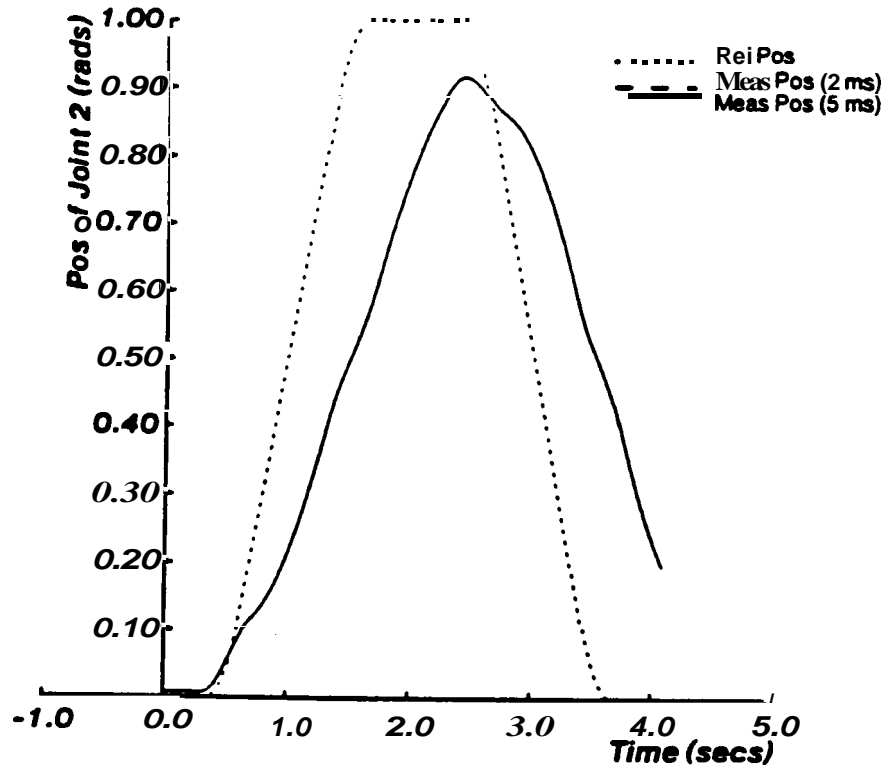


Figure 8: Performance of IJC as a Function of Sampling Period

References

1. Markiewicz, B. R., "Analysis of the Computed-Torque Drive Method and Comparison with the Conventional Position Servo for a Computer-Controlled Manipulator", Technical Memorandum **33-601**, Jet Propulsion Laboratory, Pasadena, CA, March **1973**.
2. Luh, J. Y. S., Walker, M. W. and Paul, R. P., "Resolved-Acceleration Control of Mechanical Manipulators", *IEEE Transactions on Automatic Control*, Vol. **25**, No. 3, June **1980**, pp. **468-474**.
3. Bejczy A. K., "Robot Arm Dynamics and Control", Technical Memorandum **33-669**, Jet Propulsion Laboratory, Pasadena, CA, February **1974**.
4. Khosla, P. K. and Kanade, T., "Real-Time Implementation and Evaluation of Model-Based Controls on CMU DD **ARM II**", **1986 IEEE International Conference on Robotics and Automation**, Bejczy, A. K.,ed., IEEE, April **7-10 1986**.
5. Leahy, M. B., Valavanis, K. P. and Saridis, G. N., "The Effects of Dynamics Models on Robot Control", *Proceedings of the 1986 IEEE Conference on Robotics and Automation*, IEEE, San Francisco, CA, April **1986**.
6. An, C. H., Atkeson, C. G. and Hollerbach, J. M., "Experimental Determination of the Effect of Feedforward Control on Trajectory Tracking Errors", *Proceedings of 1986 IEEE Conference on Robotics and Automation*, Bejczy, A. K.,ed., IEEE, San Francisco, **CA**, April **7-10 1986**, pp. **55-60**.
7. Schmitz, D., Khosla, P. K. and Kanade, T., "Development of CMU Direct-Drive Arm **II**", *Proceedings of the 15-th International Symposium on Industrial Robotics*, Hasegawa, Yukio,ed., Tokyo, Japan, September, **11-13 1985**.
8. Kanade, T., Khosla, P. K. and Tanaka, N., "Real-Time Control of the CMU Direct Drive Arm **II** Using Customized Inverse Dynamics", *Proceedings of the 29th IEEE Conference on Decision and Control*, Polis, M. P.,ed., Las Vegas, NV, December **12-14, 1984**, pp. **1345-1352**.
9. Khosla, P. K. and Kanade, T., "Parameter Identification of Robot Dynamics", *Proceedings of the 24-th CDC*, Franklin, G. F.,ed., Florida, December **11-13 1985**, pp. **1754-1760**.
10. Khosla, P. K., "Estimation of Robot Dynamics Parameters: Theory and Application", *Proceedings of the Second International IASTED Conference on Applied Control and Identification*, ACTA Press, Los Angeles, **CA**, December **10-12 1986**.
11. Khosla, P. K. and Kanade, T., "Experimental Evaluation of the Feedforward Compensation and Computed-Torque Control Schemes", *Proceedings of the 1986 ACC*, Stear, E. B.,ed., AAAC, Seattle, WA, June **18-20 1986**.
12. Raibert, M. H., "Analytical Equations vs. Table Lookup for Manipulation: A Unifying Concept", *Proceedings of the IEEE Conference on Decision and Control*, New Orleans, La., December **1977**, pp. **576-579**.

13. Hollerbach, J. M. and Sahar, G., "Wrist Partitioned Inverse Kinematic Accelerations and Manipulator Dynamics", *Proceedings of the First International IEEE Conference on Robotics*, Paul, R. P., ed., Atlanta, GA, March 13-15, 1984, pp. 152-161.
14. Khosla, P. K. and Neuman, C. P., "Computational Requirements of Customized Newton-Euler Algorithms", *Journal of Robotic Systems*, Vol. 2, No. 3, Fall 1985, pp. 309-327.
15. Seraji, H., "Linear Multivariable Control of Robot Manipulators", *Proceedings of the IEEE International Conference on Robotics and Automation*, IEEE, San Francisco, CA, April 1986, pp. 565-571.
16. Lee, C. S. G., Chung, M. J. and Lee, B. H., "Adaptive Control for Robot Manipulators in Joint and Cartesian Coordinates", *Proceedings of the First International IEEE Conference on Robotics*, Paul, R. P., ed., Atlanta, GA, March 13-15, 1984, pp. 530-539.
17. Takesaki, M. and Arimoto, S., "Adaptive Trajectory Control of Manipulators", *International Journal of Control*, Vol. 34, 1981, pp. 201-217.
18. Slotine, J.-J. E and Coetsee, J. A., "Adaptive Sliding Controller Synthesis for Nonlinear Systems", *International Journal of Control*, 1986.
19. Tourassis, V. D., "Computer Control of Robotic Manipulators using Predictors", *Proceedings 1987 Symposium on Intelligent Control*, IEEE, Philadelphia, PA, January 1987, pp. 204-209.
20. Astrom, K. J. and Wittenmark, B., *Computer Controlled Systems: Theory and Design*, Prentice-Hall, Englewood Cliffs, N. J., Information and System Science Series, 1984.
21. Asada, H. and Kanade, T., "Design of Direct Drive Mechanical Arms", *Journal of Vibration, Stress, and Reliability in Design*, Vol. 105, No. 1, July 1983, pp. 312-316.